



# Effect of processing conditions on electromagnetic shielding and electrical resistivity of injection-molded polybutylene terephthalate compounds

Luis C. Martins<sup>1</sup>  | Carlos N. Barbosa<sup>2</sup> | Susana Silva<sup>2</sup> | Pedro Bernardo<sup>2</sup> | Gustavo R. Dias<sup>1</sup> | António J. Pontes<sup>1</sup> 

<sup>1</sup>IPC – Institute for Polymers and Composites, University of Minho, Guimarães, Portugal

<sup>2</sup>Bosch Car Multimedia, Braga, Portugal

## Correspondence

Luis C. Martins, IPC – Institute for Polymers and Composites, University of Minho, Guimarães, Portugal.  
Email: luis.martins@dep.uminho.pt

## Funding information

European Structural and Investment Funds, Operational Competitiveness and Internationalization Program, Grant/Award Number: POCI-01-0247-FEDER-002797

## Abstract

This research introduces an analysis of the anisotropic electrical resistivity (ER) and its relation to the electromagnetic shielding effectiveness (EMSE) for two injection-molded carbon-fiber-reinforced polybutylene terephthalates (PBTs). The properties were measured for 2-mm thick injection moldings considering the effect of melt temperature, injection velocity, and flow distance. The results for one compound showed an EMSE in the range of 30–40 dB, while EMSE for a compound with lower filler content is in the range of 45–75 dB. A combination of higher temperature and higher velocity leads to an increase of EMSE for both compounds in the range of 3%–8.5%. However, the increase in flow path reduced the EMSE for both compounds up to 10%. A novel experimental apparatus was used to measure the anisotropic ER in the three directions, that is, parallel, perpendicular, and transversal to flow. It is evident that injection molding induced high anisotropy for both compound specimens, and, depending on the processing conditions, produced similar longitudinal resistivity (0.2–4  $\Omega$ .cm) but higher transversal resistivity (8–22  $\Omega$ .cm). ER properties were compared with EMSE, evidencing an inverse relation as expected. Furthermore, it was found that the longitudinal resistivity is the main contributor to the specimens shielding.

## KEYWORDS

composites, conducting polymers, electrical resistivity, electromagnetic shielding, injection molding

## 1 | INTRODUCTION

Current market trends for lightweight and innovative products stimulate a redesign and manufacture of electronic enclosures fully made of thermoplastic-based materials. These plastic enclosures need to encompass the right combination of material properties with specific design for mechanical, thermal, and electrical performance, maintaining or improving the electromagnetic

compatibility (EMC). Such solution must comply with the applicable norms and requirements of the targeted multimedia system and surpass the traditional metal-based solution by reducing the product weight and lowering the cost.

EMC is a field of science and engineering, which aims to establish guidelines for the design and operation of electrical and electronic devices in order to control the level of electromagnetic interference (EMI). These guidelines

assure that the device operates properly in its intended electromagnetic environment in such a manner that it does not interfere with other devices or itself and it is not susceptible to radiation from other devices or electrostatic discharge (ESD).<sup>[1,2]</sup>

EMI is a process where disruptive electromagnetic energy is transmitted from one electronic device to another via radiated or conducted paths or both. Such phenomenon occurs in the presence of three components: A source or emitter of interference; a receptor or victim of interference; and a propagation or coupling path between the source and the suscepter along which the energy is transferred. The most efficient way to control EMI is by a suppression process by means of a shield or filter. In these approaches, EMI shielding is the most important and effective method in the EMC design of an enclosure, and it works by reducing or eliminating EMI energy by cutting the propagation path with an EMI impermeable material (shield) to form a Faraday cage.<sup>[2]</sup>

The use of thermoplastics compounds reinforced with carbon fiber is very appealing as it allows many improvements over traditional conductive materials used for the enclosure components, such as oxidation and corrosion resistance, lower weight, and better versatility and processability, which help to consolidate the housing and reduce or eliminate seams.<sup>[3,4]</sup>

The general concept for EMC and EMI shielding is well documented for both theoretical and practical physics.<sup>[1,2,5]</sup> The shielding effectiveness (SE) of an enclosure or shield to attenuate EMI radiation is an EM field ratio between the source and the receptor that can quantify the shield efficiency to attenuate the propagation of waves through the material or apertures of an enclosure and is expressed in decibel (dB).<sup>[3,6,7]</sup> Commercial electronics typically requires an EMI-SE ranging from 40 to 60 dB, meaning that there is a 99%–99.9% attenuation of the EM field.<sup>[8,9]</sup> However, an SE of 30 dB is also considered an adequate level of shielding for many applications.<sup>[10,11]</sup>

EMI-SE is a complex problem that depends on the source type, distance, frequency of interference, waveform, shield thickness, apertures design, and shield material EM properties (electrical conductivity –  $\sigma$ ; electrical permittivity –  $\epsilon$ ; and magnetic permeability –  $\mu$ ).<sup>[1–3,6,7]</sup> However, in a simplified way, SE can be described by Schelkunoff's isomorphic and homogeneous model, stating that plane waves shielding is the sum of three mechanisms, reflection loss, absorption loss, and multiples internal reflections losses (or gains). This theory is based on three characteristics of the shield material: intrinsic impedance, skin-depth, and thickness.<sup>[3,6,10,12]</sup> Accordingly, the electromagnetic SE of a given material will

be higher as lower the respective impedance and skin-depth, and will increase proportionally to its thickness.

The methods used to measure the effectiveness of a shield are diverse but well standardized depending on the product to be measured and the type of EM source. Regarding the measurements for materials to normally incidents plane waves (far-field radiation), the most used technique is based on the procedure according to ASTM D4935 standard test method for “Measuring the Electromagnetic Shielding Effectiveness of Planar Materials.” This test method is based on the insertion loss (IL) between an EM signal generator and a receiver through a coaxial transmission line, and it is used to measure the material shielding due to EM plane waves in the far-field region. This procedure applies to the measurement of the SE of planar materials under normal incident plane waves conditions (E and H tangential to the surface of the material) according to the transverse electromagnetic (TEM) wave propagation mode. IL data and subsequent SE depend on both material's electrical and physical properties and on the measuring system itself, and it can be conveniently measured by the transmission scattering parameters ( $S_{21}$ ) using a vector network analyzer. In this proceeding, the material SE is expressed by the ratio between a reference specimen ( $S_{21\text{ref}}$ ) and a load specimen ( $S_{21\text{load}}$ ).<sup>[7,13–15]</sup>

$$\text{EMSE} = 20\log_{10} \frac{E_{\text{in}}}{E_{\text{out}}} \text{ (dB)}; \text{EMSE} = 20\log_{10} \frac{S_{21\text{ref}}}{S_{21\text{load}}} \text{ (dB)}. \quad (1)$$

From the electromagnetic theory, it is well known and documented that the scattering of an EM wave through a medium (shield) is directly proportional to the electrical conductivity of the medium. As previously mentioned, the SE of an isotropic and homogeneous material to a normally incident plane wave (far-field region) is, essentially, the sum of reflection and absorption losses through the medium. After some mathematical simplifications, one can describe the theoretical SE and its dependence on conductivity and other coefficients as follow<sup>[2]</sup>:

$$\text{EMSE} = 10\log \frac{\sigma + 2\pi f \epsilon_0 \epsilon_r}{2\pi f \mu_r \epsilon_0} - 12,04 + 8,69t \sqrt{\pi f \mu_0 \mu_r \sigma} \text{ (dB)}, \quad (2)$$

where  $f$  is the frequency of interference,  $t$  is the shield thickness,  $\sigma$  is the shield electrical conductivity,  $\epsilon_0$  is the electrical permittivity of vacuum,  $\epsilon_r$  is the relative electrical permittivity of the shield material,  $\mu_0$  is the magnetic permeability of vacuum, and  $\mu_r$  is the relative magnetic

permeability of the shield. Analyzing this equation, it is possible to see that SE is proportional to the shield conductivity, wherein the reflection is proportional to the conductivity logarithm, while the absorption is proportional to the square root of conductivity. Accordingly, it is perfectly understandable that metals are the most used materials to shield electronic devices from EMI radiations. If a 0.5 mm copper foil is considered to shield a 1 GHz signal source, according to this theoretical model, it should expect a SE of 285 dB. However, polymeric compounds have a much more limited conductivity, which introduces a higher challenge for their implementation as a replacement to metallic EMI shields. Nevertheless, according to this equation, if the plastic composite can be optimized to achieve a modest conductivity of 200 S/m, it should provide a theoretical shielding of 30 dB for a 1 mm thick part, which can be adequate for some cases.

As plastic composites can provide great advantages, considerable efforts have been made by researchers and institutions to comprehend and optimize their electrical conductivity and/or electromagnetic shielding. The polymer matrix can be reinforced by dispersed electrically conductive fillers, such as carbon materials (carbon fibers, carbon black, CNT, graphene) or metallic (stainless steel, copper, or aluminum) particles or fibers, creating traditional composite materials or more complex and futuristic structures with a wide range of properties, from antistatic to conductive.<sup>[3,6,7,12,16–27]</sup>

One advantage of reinforced thermoplastic composites is their process flexibility and possibility to fit, and control, the electrical properties, in particular the EM shielding, to a specific need by manipulating some factors along the manufacturing line. The main factors to control are the material composition (type of filler, its length or aspect ratio, and its volume fraction), the part thickness, and the processing parameters that will affect the filler dispersion and orientation.<sup>[27–30]</sup>

Weber et al., verified that the electrical resistivity (ER) of polypropylene reinforced with nickel-coated graphite (NCG) fibers or stainless steel (SS) fibers is anisotropic for both compression molding, injection molding and extrusion samples, being lowest in the main direction of fiber orientation. Additionally, besides checking that the distance to the injection gate influences the measured resistivity, they found that the resistivity decreases with an increase of fiber loading and that the SS fibers percolation threshold is lower than the NCG fibers but NCG fibers provided lower resistivities at ultimate loading.<sup>[28]</sup>

Al-saleh et al. developed several investigations regarding the addition of different carbon fillers to polymeric matrixes and found that there is a direct relation between the electrical conductivity and shielding, and that these

properties are directly proportional to the filler concentration and sample thickness.<sup>[10,31–34]</sup>

Chiu et al. investigated the addition of carbon fibers to a nylon matrix in order to shield a laser diode package and, besides finding that the ER is lower with an increase of fiber loadings, they found that higher fiber lengths provided even lower resistivity. Lower resistivity leads to higher electromagnetic shielding, as they are verified. The SE at 1 GHz was almost 60 dB for a loading of 30% of long carbon fibers, while the same concentration of short carbon fibers only provided a 30 dB shielding.<sup>[35]</sup>

Arjmand et al. studied the addition of MWCNT to polycarbonate and polystyrene, produced by compression or injection molding. They found that the ER is more anisotropic in injection-molded samples, and resistivity decays with an increase of CNT loadings and a lower percolation threshold for compression molding samples. Furthermore, they measured the EM SE and found that shielding increased with an increase of injection molding temperature and velocity, but was lower than the shielding measured in compression molded samples.<sup>[36,37]</sup>

Bryant studied the addition of long nickel-coated carbon fiber (LNCCF) to polycarbonate in comparison to standard nickel-coated carbon fiber (NNCF) and stainless steel fiber (SSF) and discovered that at relatively low loading levels, the addition of LNCCF resulted in an increase in the EM SE. Hence, LNCCF is an excellent filler to use in order to achieve higher SE with lower specific gravity. Nevertheless, at a loading of 20 wt%, all of the fillers provided an excellent shielding above 80 dB for a 3 mm thick sample.<sup>[9]</sup>

The synergic effect of the addition of multi-fillers was found to be beneficial to the electrical properties and SE of the hybrid composite. The addition of carbon filler, such as CNT or carbon black, to an existing loaded polymer can provide a decrease in resistivity and, hence, an increase in SE.<sup>[8,34,38–42]</sup>

The processing parameters, specifically the injection molding variables, can affect the performance of plastic parts since the thermomechanical dynamics in the process will affect the filler dispersion and orientation. The melt temperature, mold temperature, injection velocity, holding pressure, back pressure, and screw speed are the most studied processing variables, but other parameters such as gate design and channel length. It was found, in correlation with the type of filler and concentration, that the melt temperature, holding pressure, injection velocity, and channel length can have a significant effect on the electrical conductivity and EM shielding. These factors contribute significantly to the fillers' dispersion and orientation along the sample, leading to a good or bad conductive network from the fillers inside the polymer matrix.<sup>[21,37,43–51]</sup>

As discussed, there is considerable know-how about the electrical and electromagnetic properties of polymers reinforced with electrically conductive fillers. Nevertheless, such materials have complex behavior and need sensitive control to optimize the final properties and costs. Therefore, this investigation aims to add value to the field of ER and electromagnetic shielding of PBT compounds reinforced with carbon fibers, specifically regarding the effect of the melt temperature, injection velocity, and flow path length on the anisotropic ER and SE of injection molding samples.

## 2 | EXPERIMENTAL WORK

### 2.1 | Materials

Two commercially available PBT thermoplastic compounds loaded with carbon-based fillers, such as carbon fibers (CF) and/or carbon black (CB), were used in this investigation. These materials are suitable for injection molding, and some of their general properties are provided in Table 1. Due to non-disclosure agreements (NDAs) with suppliers, the commercial names and filler specifications cannot be provided.

### 2.2 | Samples preparation

Test samples with dimensions of  $150 \times 80 \times 2 \text{ mm}^3$  (rectangular plates) were produced in an injection molding press (Ferromatik Milacron K85-S/2F). In this process, both thermoplastics were injected into a one-cavity mold through a 1.5 mm thick flash gate. The generic dimensions of the moldings as well as the real molded parts (including the feed system) can be found in Figure S1.

In order to check the influence of the injection molding conditions, the molded specimens were produced varying the melt temperature and the injection velocity in two levels for both compounds, one experimental condition with lower values and other condition with higher values, as shown in Table 2.

**TABLE 1** Datasheet properties of the injection molding compounds

Material	Comp#01	Comp#02
Filler composition (wt%)	20% CF + 10% CB	20% CF
Density ( $\text{g/cm}^3$ )	1.36	1.38
Tensile modulus (GPa)	12	12
Surface resistance ( $\Omega$ )	$<10^1$	$<10^3$
Conductive fillers (wt%)	$\sim 30$	$\sim 20$

The filling of the moldings was performed by determining the necessary feeding stroke to fill the cavity up to approximately 99% of its volume. Once the feeding stroke parameter has been identified, the packing phase parameters were determined. The packing pressure is generally considered as 80% of the pressure required to fill the part. Whereas the holding time was identified by sequentially increase the holding pressure time in order to identify the instant at which the part weight stabilizes, that is, the gate freezes. The actual injection molding conditions are listed in Table 3 for all production series. Once steady state conditions were achieved, 10 specimens were obtained for further investigations for both materials and experiments.

### 2.3 | Characterization

EMSE measurements were performed with a test procedure following the withdraw ASTM D4935-99 Standard (Standard Test Method for Measuring the Electromagnetic Shielding Effectiveness of Planar Materials) wherein the sample is placed between two coaxial flanges, which acts both as a sample holder and a TEM waveguide. The sample holder, which is an enlarged coaxial transmission line made in a brass alloy and was designed to support 60 mm diameter samples maintaining a characteristic impedance of  $50 \Omega$  throughout the entire length of the holder, is connected to a vector network analyzer (R&S<sup>®</sup>ZVL3) with the assistance of two coaxial cables and two 10 dB  $50 \Omega$  attenuators. EM shielding can be evaluated through the decay of the transmitted signal between the coaxial ports and referred by the VNA as S21 or S12 scattering parameter.

Tests were carried out by considering the relative location of the molding samples, that is, one observation area near gate and other at opposite gate location in order to analyze the material properties as the flow distance increase. For each experiment condition and molding location, a total of five samples were evaluated to obtain a reasonable statistical mean.

SE was measured at the frequency range between 30 MHz and 3 GHz, radio frequency spectrum common to automotive multimedia systems, and it was determined

**TABLE 2** Injection molding plan

Condition	Melt temperature ( $^{\circ}\text{C}$ )	Injection velocity (mm/s)
Exp#01	–	–
Exp#02	+	+

Material	Compound#01		Compound#02	
Work plan	Exp#01	Exp#02	Exp#01	Exp#02
Melt temperature (°C)	250	265	240	260
Injection velocity (mm/s)	50	200	60	110
Flow rate (cm <sup>3</sup> /s)	62.8	251.3	42.4	77.8
Injection pressure (bar)	1814	1828	1030	850
Holding pressure (bar)	632	632	500	500
Holding time (s)	5	5	5	5
Mold temperature (°C)	80	80	80	80
Cooling time (s)	15	15	15	15

TABLE 3 Injection molding conditions

by the ratio between reference and load samples transmission scattering coefficients (S21) as expressed in Equation (3).

$$SE = 20 \log_{10} \frac{S_{21ref}}{S_{21load}} \text{ (dB)}. \quad (3)$$

Electrical resistance was measured under ambient temperature conditions with two customized four-point copper electrodes. The four-point measurement protocol uses two electrodes to apply a direct current to the sample while the DC voltage is measured across the other two electrodes. Additionally, a power source and two multimeters for voltage and current measurements were used in the test setup. The electrical resistance is calculated for each sample using Equation (4):

$$R = \frac{V}{I}, \quad (4)$$

where  $R$  = resistance ( $\Omega$ );  $V$  = measured voltage (V);  $I$  = applied current (A).

The pair of copper electrodes for longitudinal resistivity measurements were designed based on ASTM D4496-87 (test method for DC resistance of moderately conductive materials) and ISO 3915:1981 (measurement of resistivity of conductive plastics). For the transversal resistivity, a capacitor-like geometry was manufactured with copper electrodes placed in the opposite faces. In both cases, there are independent electrodes to supply direct current and to quantify the resulting voltage.

Tests were carried out by considering the relative location of the samples, that is, positioned at near gate and at opposite gate location. For each location, three different measurements were conducted to get a comprehensive understanding of the anisotropic ER of the injection-molded plaques. The longitudinal (in-plane) ER was evaluated in two directions, that is, parallel and perpendicular to the flow direction, while the transversal

(through-plane) resistivity of the moldings was evaluated across the specimen thickness. Longitudinal and transversal resistivities were calculated using Equations (5) and (6), respectively, based on the measured electrical resistance and samples geometry.

$$\rho_l = R_l \times \frac{W \times t}{L}, \quad (5)$$

where  $\rho_l$  = longitudinal resistivity ( $\Omega \cdot \text{cm}$ );  $R_l$  = resistance ( $\Omega$ );  $W$  = width of the specimen (cm);  $t$  = specimen thickness (cm);  $L$  = length of the specimen between electrodes (cm).

$$\rho_t = R_t \times \frac{A}{t}, \quad (6)$$

where  $\rho_t$  = transversal resistivity ( $\Omega \cdot \text{cm}$ );  $R_t$  = resistance ( $\Omega$ );  $A$  = area of the electrodes ( $\text{cm}^2$ );  $t$  = distance between the electrodes or sample thickness (cm).

Tests were synchronized with a motorized test stand equipped with a digital force gauge of a maximum load capacity of 250 N to evaluate the ER of the moldings as a function of the compression force applied to the samples positioned in-between identical custom-made electrodes.

Additional information about the experimental characterization can be found in Data S1.

### 3 | RESULTS AND DISCUSSION

Before analyzing the EM shielding and ER properties of the produced compounds moldings, it is important to evidence that the measured samples have stable density values for the different injection molding conditions, while their thickness slightly increased with the increase of the melt temperature and injection velocity (Table 4).

The effect of melt temperature and injection velocity, as well as flow distance, are discussed below for both



EMSE and ER. Furthermore, moldings anisotropic resistivity is presented and its relation to the measured shielding is covered.

The results are presented in several graphical figures and further discussed in text form. However, the reader can access additional tables in Data S1.

### 3.1 | EM shielding results

The EMSE between 30 MHz and 3 GHz, automotive frequency band, was evaluated by considering the effect of injection molding conditions ( $T_i$  and  $V_i$  varied in two levels) and sample relative location (near and opposite gate). The average results at specific frequencies are shown in Figures 1 and 2, for Compound#01 and

Compound#02, respectively. The coordinate axes of the plots were scaled for improved results observation.

For the observed frequency band, Compound#01 shielding was measured in the 30–40 dB range, while shielding measures for Compound#02 was in the 45–75 dB range. Therefore, despite having lower conductive filler content (less 10%), Compound#02 showed about 13–30 dB improved performance when compared with Compound#01, depending on the frequency band and injection molding conditions.

As expected, and projected in theoretical models, the EM shielding increases with the increase of frequency, since the wavelength becomes relatively smaller compared with the specimen's thickness and conductive fillers dimensions. As smaller the wavelength is, the bigger will become the EM attenuation due to absorption

TABLE 4 Specimens physical properties

Material	Compound#01		Compound#02	
Work plan	Exp#01	Exp#02	Exp#01	Exp#02
Average thickness (mm)	1.93	2.05	1.95	1.99
Part density ( $\text{g}/\text{cm}^3$ )	1.32	1.32	1.34	1.35

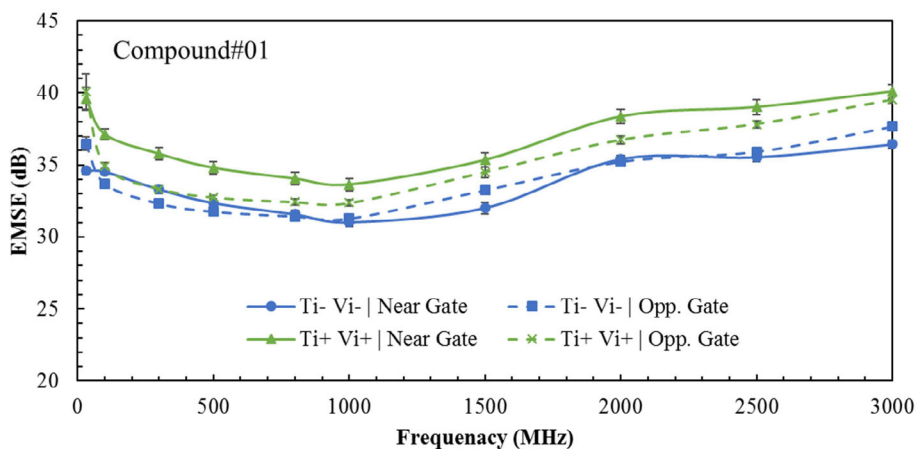


FIGURE 1 EM shielding for Compound#01

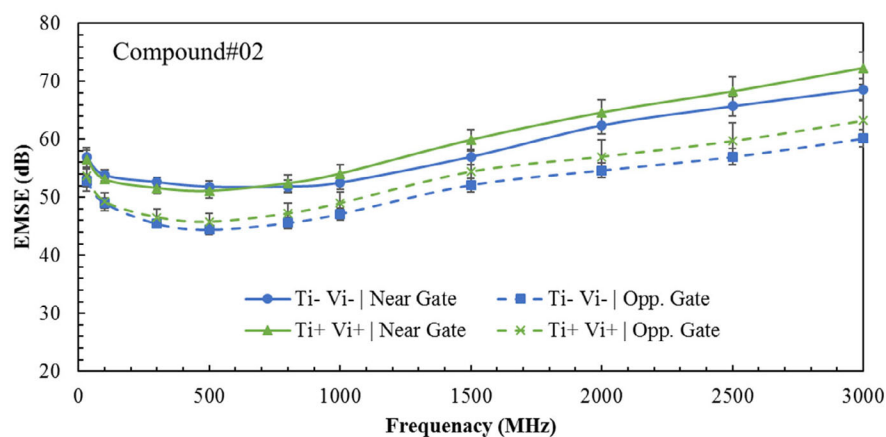


FIGURE 2 EM shielding for Compound#02

effect through the material. Below 1 GHz, there is an apparent increase of shielding for lower frequencies, but that's not an effect from the material but an effect of the impedance mismatch in the experimental setup.

Looking further into these results, it is possible to see a distinction in the EM shielding for the different injection molding conditions (Ti and Vi varied in two levels) and sample relative location (near and opposite gate). Depending on the observed frequency, the increase of the injection molding conditions promoted an increase of the material's SE of 1–5 dB and 0.5–3.5 dB for Compound#01 and Compound#02, respectively. Therefore, the contribution of the injection molding conditions for material EMSE appears to be flat and insignificant. However, the higher observed variations can be in the order of 15% for Compound#01 and 5% for Compound#02, which shows that Compound#01 is more affected by processing conditions while Compound#02 properties are more stable to the change in parameters. Regarding the effect of the flow distance (relative sample position), the increase of the distance leads to a maximum shielding decrease of 2.5 dB (6.8%) for Compound#01 and a maximum decrease of 9 dB (12.5%) for Compound#02. Therefore, the properties for Compound#01 are more consistent along the flow course than those measured for Compound#02.

The effects of the injection molding conditions and flow distance can be better observed in Figure 3 (and Table S1), which shows the EMSE at 1 GHz for both compounds and for the two experimental conditions and two measurement areas (near and opposite to gate).

At 1 GHz, frequency that is generally used by manufacturers to disseminate their material's shielding, it is possible to see that the measured shielding is almost constant for different injection molding conditions, as previously mentioned. However, a more accurate eye can notice a small increase of shielding with the increase of

the processing conditions. The increase for Compound#01 was in the order of 2.63 dB (8.5%) near the gate location and 1.09 dB (3.5%) at opposite from gate location, while the increase for Compound#02 was in the order of 1.53 dB (2.9%) near the gate location and 1.85 dB (3.9%) at opposite from gate location. Therefore, the increase of injection molding conditions was somewhat more beneficial for Compound#01 than for Compound#02 as the resultant shielding was slightly more improved for Compound#01.

Regarding the relative sample position, which is a way to analyze the effect of the flow distance on the material shielding, it is possible to see some mixed results for Compound#01 and an evident decrease of shielding for Compound#02. For the lower injection molding conditions (Exp#01), it is possible to see a slight shielding improvement of 0.26 dB (0.8%) for Compound#01 and a shielding decay of 5.4 dB (10.3%) for Compound#02. For the higher injection molding conditions (Exp#02), it is more noticeable a shielding decay of 1.28 dB (3.8%) and 5.08 dB (9.4%) for Compound#01 and Compound#02, respectively. Hence, this study shows that the increase of the flow length promotes a decay of the material shielding and that Compound#02 can be a better material for long flow parts as it appears to have more stable properties along the flow of the injection-molded part.

### 3.2 | Electrical resistivity

The ER was evaluated considering the effect of injection molding conditions (Ti and Vi varied in two levels), sample relative location (near and opposite gate), and applied compression force, ranging from 20 to 200 N. The ER was measured in both in-plane/longitudinal (parallel and perpendicular to flow) and through-plane (transversal to flow directions).

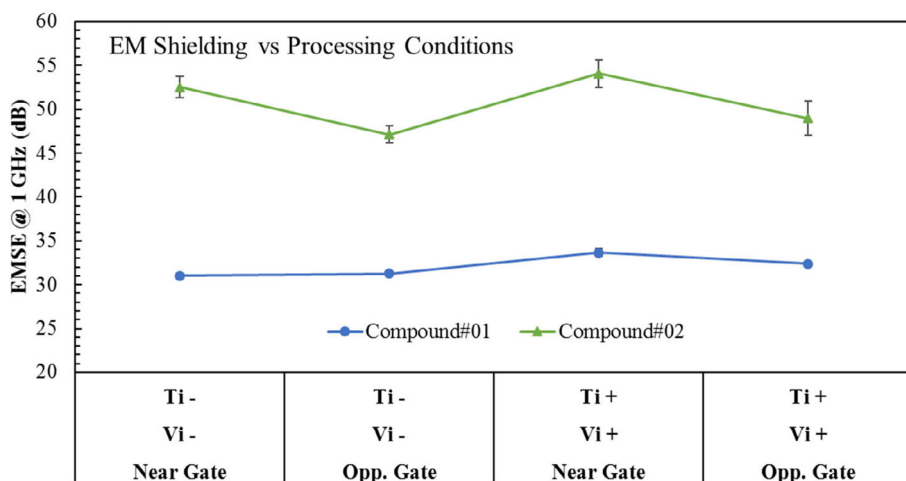


FIGURE 3 Effect of processing conditions on the EM shielding for both compounds

The mean ER results for both compounds are presented as a function of the compression force for the two experimental conditions and the two selected sample relative locations, according to the experimental protocol previously described. ER results are shown in Figures 4–6 for parallel to flow, perpendicular to flow, and transversal to flow measurements, respectively. A logarithmic scale was applied to the y-coordinate axes of the plots for better comparison.

It is possible to see that the ER for Compound#01 was measured in the range of 1–5  $\Omega\cdot\text{cm}$  for parallel to flow direction, 1–4  $\Omega\cdot\text{cm}$  for perpendicular to flow direction, and 10–40  $\Omega\cdot\text{cm}$  for transversal to flow direction. While ER measures for Compound#02 were in the range of 0.2–0.8  $\Omega\cdot\text{cm}$  for parallel to flow direction, 0.2–0.6  $\Omega\cdot\text{cm}$  for perpendicular to flow direction, and 10–35  $\Omega\cdot\text{cm}$  for transversal to flow direction. Therefore, as previously reported on the EMSE results analysis, despite having lower conductive filler content (less 10%), Compound#02 has longitudinal resistivities (parallel and perpendicular to flow) that are approximately one order of magnitude lower than resistivities measured for Compound#01.

However, transversal resistivities do not have the same ratio and in fact are quite similar since both are in the range between 10 and 40  $\Omega\cdot\text{cm}$ .

Furthermore, it is possible to see the anisotropic behavior of these compounds on the transversal direction, since for both compounds, the ER resistivity is similar for parallel and perpendicular to flow directions (homogeneous in-plane) but it is about  $\times 10$  and  $\times 100$  higher in the transversal direction (heterogeneous through-plane) for Compound#01 and Compound#02, respectively.

As previously mentioned, the acquisition of the ER was executed with different compression force, which was applied on the top electrode. Observing the ER charts, from Figures 4 to 6 and the Table S2, the obtained results show, with some exceptions to the norm (red), that an increase of compression force from 20 N to 200 N led to a decrease of electrical down to 60% for some samples. The probable explanation for this effect is the increase of the contact area between the copper electrodes and the specimen surface area and/or specimen squeeze with the increased force creating new conductive

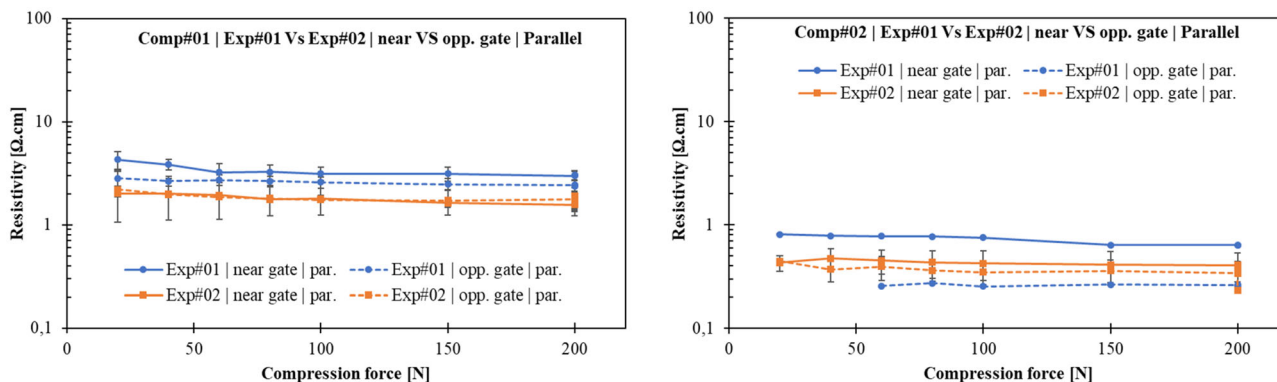


FIGURE 4 Parallel resistivity in function of applied compression force. Results for Compound#01 (left) and Compound#02 (right) for different processing conditions and sample locations

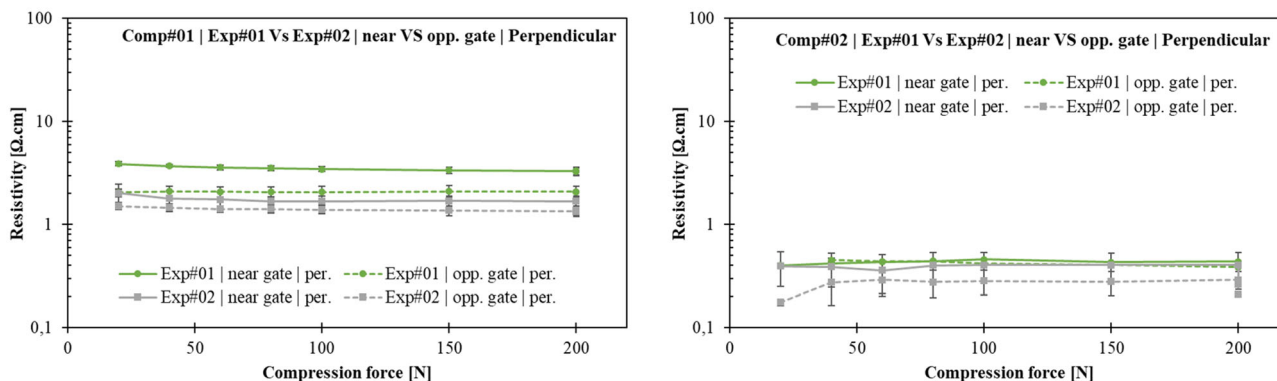


FIGURE 5 Perpendicular resistivity in function of applied compression force. Results for Compound#01 (left) and Compound#02 (right) for different processing conditions and sample locations



networks.<sup>[52]</sup> The fact that the compression force induces higher variations on the transversal measurements (between 30% and 60% points) support this hypothesis.

The effects of the injection molding conditions and sample relative location can be better observed in Figure 7, as well as Tables S3 and S4, which shows the electrical resistivities at 200 N applied compression force for both compounds and for the two experimental conditions and two specimen areas (near and opposite to gate).

As previously mentioned, the ER resistivity is similar for parallel and perpendicular to flow directions, being below 5  $\Omega\cdot\text{cm}$  for Compound#01 and less than 0.8  $\Omega\cdot\text{cm}$  for Compound#02. While the Transversal ER for both compounds, being those 10x and 100x higher than the longitudinal resistivity for Compound#01 and Compound#02, respectively. Therefore, it is possible to confirm the anisotropic behavior of both materials. However, there is a great deviation on the transversal results induced by errors on the experimental apparatus.

As it was observed in the EM shielding performance, both compound's ER changes with the increase of the

injection molding conditions and the relative position of measurement. However, these variations are not completely in agreement with the variation observed in EMSE results (This subject will be discussed in the next section).

For Compound#01, the increase of injection molding parameters induced a decrease of specimen resistivity in the parallel and perpendicular directions and increased in the transversal direction. ER variations for the parallel direction measures was in the order of 1.2  $\Omega\cdot\text{cm}$  (43.1%) near the gate location and 0.41  $\Omega\cdot\text{cm}$  (18.9%) at opposite from gate location. The ER decreases in perpendicular direction in the order of 1.41  $\Omega\cdot\text{cm}$  (45.2%) near the gate location and 0.52  $\Omega\cdot\text{cm}$  (27.6%) at opposite from gate location. As opposed to the others, the ER increased in transversal direction in the order of 0.69  $\Omega\cdot\text{cm}$  (5.1%) near the gate location and 7.63  $\Omega\cdot\text{cm}$  (73.8%) at opposite from gate location. Regarding the flow distance effect, the increase in distance (from near gate to opposite from gate) induced an average decrease of specimen resistivity, with two of the measures breaking the trend and showed

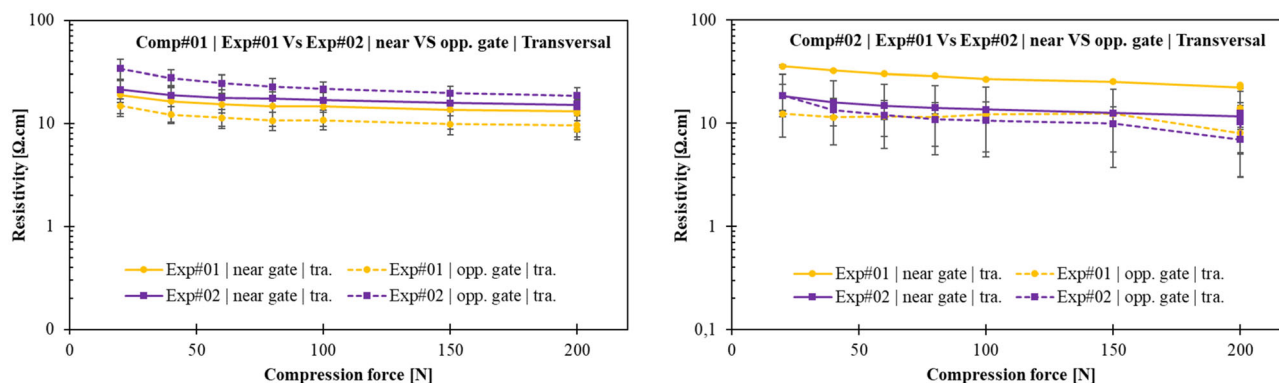


FIGURE 6 Transversal resistivity in function of applied compression force. Results for Compound#01 (left) and Compound#02 (right) for different processing conditions and sample locations

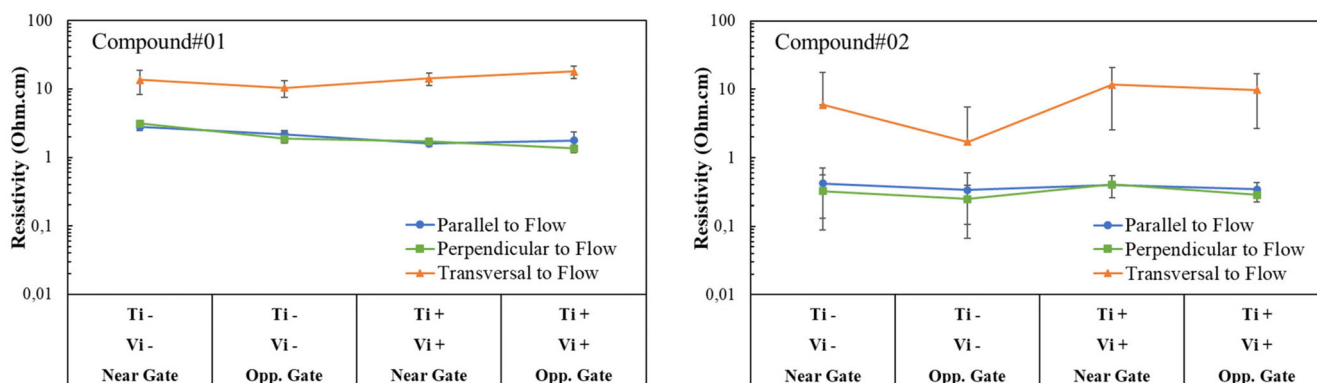


FIGURE 7 Electrical resistivity at 200 N compression force. Results for Compound#01 (left) and Compound#02 (right) for different processing conditions, sample locations, and measurement setup

increased resistivity. The ER in the parallel direction decreased in the order of 0.62  $\Omega\cdot\text{cm}$  (22.3%) for samples produced in the Exp#01 conditions and increased 0.17  $\Omega\cdot\text{cm}$  (10.9%) for samples produced in Exp#02 conditions. The ER in the perpendicular direction decreased in the order of 1.26  $\Omega\cdot\text{cm}$  (40.2%) and decreased 0.36  $\Omega\cdot\text{cm}$  (21.0%) for samples produced in Exp#01 and Exp#02 conditions, respectively. The ER in the transversal direction decreased in the order of 03.19  $\Omega\cdot\text{cm}$  (23.5%) for samples produced in the Exp#01 conditions and increased 3.76  $\Omega\cdot\text{cm}$  (26.5%) for samples produced in EXP#02 conditions, respectively.

For Compound#02, the effect of the injection molding parameters increase was essentially opposed to those obtained for Compound#01 since it induced an increase of the specimen resistivity in the three measurement directions (parallel, perpendicular, and transversal), with only one measurement resulting in the ER decrease. For the parallel to flow samples, measures showed an insignificant variation, being that it only decreased 0.02  $\Omega\cdot\text{cm}$  (4.3%) near the gate location and only increased 0.01  $\Omega\cdot\text{cm}$  (3.1%) at opposite from gate location. In perpendicular to flow samples, the ER increased in the order of 0.08  $\Omega\cdot\text{cm}$  (23.7%) near the gate location and 0.04  $\Omega\cdot\text{cm}$  (14.5%) at opposite from gate location. The transversal to flow ER also increased in the order of 5.77  $\Omega\cdot\text{cm}$  (97.6%) near the gate location and a shocking 8.15  $\Omega\cdot\text{cm}$  (476.9%) at opposite from gate location. Regarding the flow distance effect, the results showed a decrease of ER with the increase in distance (from near gate to opposite from gate). The ER in the parallel direction decreased in the order of 0.09  $\Omega\cdot\text{cm}$  (20.3%) for samples produced in Exp#01 conditions and 0.06  $\Omega\cdot\text{cm}$  (14.1%) for samples produced in Exp#02 conditions. At the perpendicular direction, the ER decreased in the order of 0.08  $\Omega\cdot\text{cm}$  (23.6%) and 0.12  $\Omega\cdot\text{cm}$  (29.3%) for samples produced in Exp#01 and Exp#02 conditions, respectively. The ER

in the transversal direction also decreased 4.20  $\Omega\cdot\text{cm}$  (71.1%) for samples produced in Exp#01 conditions and 1.83  $\Omega\cdot\text{cm}$  (15.6%) for samples produced in EXP#02 conditions, respectively.

### 3.3 | ER and EMSE relations

The EM wave scattering on a homogeneous and isotropic medium (or material) is related to the intrinsic impedance of the actual medium. This wave impedance is influenced by the electrical permittivity, magnetic permeability, and electrical conductivity of the medium it travels through. Hence, the EMSE of the material is proportional to the electrical conductivity (EC) and has a logarithmic growth when conductivity increases.

In this section, we compare the measured EMSE with the corresponding measured ER. The direction of measurement, if parallel, perpendicular, or transversal to injection molding flow, was considered in this analysis. In Figure 8, it is possible to see the measured EMSE for both compounds (plus one more) and the corresponding measured ER. Additionally, the theoretical curve for the expected EMSE for an isotropic and homogeneous material with a given constant EC (or ER) was also charted for comparison with the experimental results.

As expected, both experimental and theoretical data show that EMSE increases with lessening of ER, being that at an exponential rate.

Furthermore, it is possible to see that the parallel and perpendicular conductivities (or ER) are in a closer range and closer to the theoretical dots. Therefore, one can affirm that the primary contributor for molding EMSE is the longitudinal (in-plane) resistivity, since it fit better with the theoretical prediction.

An important point to take from this analysis is that somehow the experimental values of conductivity are

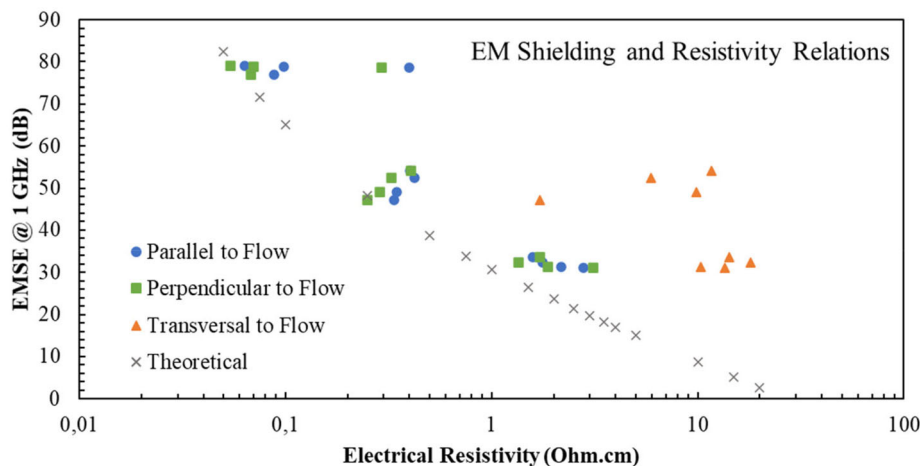


FIGURE 8 EMSE relation with both experimental (parallel, perpendicular and transversal to flow) and theoretical ER. ER axis is plotted with a logarithmic scale

likely to have been underestimated. The reason is that almost all the measured values for the EC are above the theoretical values (or to the left of the trend line).

As previously mentioned, the change in ER with the variation of experimental conditions and sample relative position (near gate and opposite to gate) is not completely in agreement with the variation observed in EMSE results. These results are discussed below and are based on the collected data placed in Tables S1, S3, and S4.

As can be observed, the EMSE for both compounds increases with the increase of the injection molding conditions (Exp#01  $\rightarrow$  Exp#02), up to 8.5% for Compound#01 and 3.9% for Compound#02. Regarding the ER results, it is possible to observe that, for Compound#01, the effect of the injection molding conditions' increase agrees with the EMSE results, since ER decreased in the longitudinal direction (18.9%–45.2%). However, experimental results showed that increasing the injection conditions for Compound#02 resulted on an EMSE improvement but an opposing increase in ER for almost all the specimens.

Regarding the effect of relative distance increase, the results of ER for Compound#02 are once again in non-conformity with the corresponding EMSE results, since the EMSE decreased but near 10% while the ER also decreased more than 14% (Note: EMSE is inversely proportional to ER). For Compound#01, the relation between EMSE and ER results is slightly in agreement. For Exp#01, there was a decrease in ER for all samples and a corresponding increase of EMSE (almost constant). While for Exp#02, there was an EMSE decrease of 3.8%, but the ER is not in total conformity since the ER in the perpendicular to flow direction also decreased 21%, as opposing to the correct trend obtained by ER in the parallel and transversal directions.

## 4 | CONCLUSIONS

The ER and EMI-SE of two high-performance PBT-based injection-molded thermoplastic compounds were evaluated by considering different processing settings and sample measurements relative location. The shielding for Compound#01 was in the range of 30–40 dB while, despite having lower filler content, shielding performance for Compound#02 was in the range of 45–75 dB. These results evidence the importance of selecting an adequate filler material for the required properties.

The ER (longitudinal and through-thickness) was also examined as a function of the applied compression force. Generally, an increase in force leads to lower resistivity.

The ER values at the longitudinal direction (parallel and perpendicular) are in the same magnitude order and are the primary contributors for moldings shielding since they fit better with the theoretical predictions, obtained from Equation (2). Hence, the ER at the longitudinal direction is lower than the measured at the transversal direction for both compounds and it is of about  $\times 10$  and  $\times 100$ , respectively. At a macro level, it is possible to see that ER values agree with the macro EMSE magnitudes, being that the average longitudinal ER for Compound#01 is in the range of 1–4  $\Omega\cdot\text{cm}$  and for Compound#02 is in the range of 0.2–0.8  $\Omega\cdot\text{cm}$ , which explains the better EMSE performance of Compound#02.

Doing a more accurate analysis, it was observed that the change in ER (or EC) with the variation of injection molding conditions and sample relative position (near gate and opposite to gate) is not completely in agreement with the variation observed in EMSE results. Also, the adopted ER setup, which is a novel procedure, provides average results with high deviations, especially for the through-thickness measures. Therefore, an improvement of the experimental proceedings is recommended.

The authors would like to provide an analysis of the filler concentration and dispersion through microstructure observation to support the measured EMSE and ER results. Unfortunately, measurements could not be made as part of the project.

## ACKNOWLEDGMENTS

The authors would like to acknowledge all the associates from University of Minho, Centre for Innovation in Polymer Engineering (PIEP and Bosch Car Multimedia who had an active part in the development of this research and acknowledge that this project, INNOVCAR, was supported by the European Structural and Investment Funds in the FEDER component, through the Operational Competitiveness and Internationalization Program (COMPETE 2020) [Project no 002797; Funding Reference: POCI-01-0247-FEDER-002797].

## ORCID

Luis C. Martins  <https://orcid.org/0000-0002-8851-3665>

António J. Pontes  <https://orcid.org/0000-0002-8964-400X>

## REFERENCES

- [1] K. L. Kaiser, *Electromagnetic Compatibility Handbook*, CRC Press, Boca Raton, FL **2005**.
- [2] X. C. Tong, *Advanced Materials and Design for Electromagnetic Interference Shielding*, CRC Press, Boca Raton, FL **2009**.
- [3] D. D. Chung, *Carbon* **2001**, 39, 279. [https://doi.org/10.1016/S0008-6223\(00\)00184-6](https://doi.org/10.1016/S0008-6223(00)00184-6)

- [4] M. H. Al-Saleh, U. Sundararaj, *Macromol. Mater. Eng.* **2008**, 293, 621. <https://doi.org/10.1002/mame.200800060>
- [5] V. P. Kodali, *Engineering Electromagnetic Compatibility: Principles, Measurements, and Technologies*, IEEE Press, New York, NY **1996**.
- [6] D. Jiang, V. Murugadoss, Y. Wang, J. Lin, T. Ding, Z. Wang, Q. Shao, C. Wang, H. Liu, N. Lu, R. Wei, A. Subramania, Z. Guo, *Polym. Rev.* **2019**, 59, 280. <https://doi.org/10.1080/15583724.2018.1546737>
- [7] S. Geetha, K. K. S. Kumar, C. R. K. Rao, M. Vijayan, D. C. Trivedi, *J. Appl. Polym. Sci.* **2009**, 112, 2073. <https://doi.org/10.1002/app>
- [8] N. Bryant. EMI Shielding Effects of Carbon Nanotubes on Traditional EMI Plastics, presented at IEEE International Symposium on Electromagnetic Compatibility (EMC), **2010**, pp. 194–197.
- [9] N. Bryant. Using Long Fiber Nickel Coated Carbon Fiber (LFNCCF) to produce Light Weight EMI Shielding Plastic Composites, **2013**.
- [10] M. H. Al-Saleh, U. Sundararaj, *Carbon* **2009**, 47, 1738. <https://doi.org/10.1016/j.carbon.2009.02.030>
- [11] C. Morari, I. Balan, J. Pintea, E. Chitanu, I. Iordache, *Prog. Electromagn. Res. M* **2011**, 21, 93. <https://doi.org/10.2528/PIERM11080406>
- [12] P. Saini, M. Arora, *New Polymers for Special Applications* (Ed: A. S. Gomes), InTechOpen, London **2012**, p. 71.
- [13] ASTM International. ASTM D 4935 - Standard Test Method for Measuring the Electromagnetic Shielding Effectiveness of Planar Materials, *10*, pp. 1–10, **1999**.
- [14] M. S. Sarto, A. Tamburrano, *IEEE Trans. Electromagn. Compat.* **2006**, 48, 331. <https://doi.org/10.1109/TEMC.2006.874664>
- [15] H. Vasquez, L. Espinoza, K. Lozano. Simple Device for Electromagnetic Interference Shielding Effectiveness Measurement, presented at IEEE, pp. 62–68, **2009**.
- [16] S. K. H. Gulrez, M. E. A. Mohsin, H. Shaikh, A. Anis, A. M. Pulose, M. K. Yadav, E. H. P. Qua, S. M. Al-Zahrani, *Polym. Compos.* **2014**, 35, 900. <https://doi.org/10.1002/pc.22734>
- [17] M. Jouni, D. Djurado, V. Massardier, G. Boiteux, *Polym. Int.* **2017**, 66, 1237. <https://doi.org/10.1002/pi.5378>
- [18] A. Kausar, S. Ahmad, S. M. Salman, *Polym.-Plast. Technol. Eng.* **2017**, 56, 1027. <https://doi.org/10.1080/03602559.2016.1266367>
- [19] N. Bagotia, V. Choudhary, D. K. Sharma, *Polym. Adv. Technol.* **2018**, 29, 1547. <https://doi.org/10.1002/pat.4277>
- [20] P. Banerjee, Y. Bhattacharjee, S. Bose, *J. Electron. Mater.* **2020**, 49, 1702. <https://doi.org/10.1007/s11664-019-07687-5>
- [21] J. Martinsson, J. L. White, *Polym. Compos.* **1986**, 7, 302.
- [22] R. M. Simon, Emi Shielding With Conductive Plastics, presented at IEEE International Symposium on Electromagnetic Compatibility, **1983**, pp. 281–285.
- [23] B. D. Mottahed, S. Manoochchri, *Polym.-Plast. Technol. Eng.* **1995**, 34, 271. <https://doi.org/10.1080/03602559508015827>
- [24] U. Lundgren, J. Ekman, J. Delsing, *IEEE Trans. Electromagn. Compat.* **2006**, 48, 766.
- [25] A. Rahman, I. Ali, S. M. Al Zahrani, R. H. Eleithy, *Nano* **2011**, 6, 185. <https://doi.org/10.1142/S179329201100255X>
- [26] T. K. Das, S. Prusty, *Polym.-Plast. Technol. Eng.* **2012**, 51, 1487. <https://doi.org/10.1080/03602559.2012.710697>
- [27] J. M. Thomassin, C. Jérôme, T. Pardoën, C. Bailly, I. Huynen, C. Detrembleur, *Mater. Sci. Eng. R. Rep.* **2013**, 74, 211. <https://doi.org/10.1016/j.mser.2013.06.001>
- [28] M. Weber, M. R. Kamal, *Polym. Compos.* **1997**, 18, 726. <https://doi.org/10.1002/pc.10325>
- [29] A. Ameli, M. Nofar, S. Wang, C. B. Park, *ACS Appl. Mater. Interfaces* **2014**, 6, 11091–11100.
- [30] S. Mondal, R. Ravindren, B. Shin, S. Kim, H. Lee, S. Ganguly, N. C. Das, C. Nah, *Polym. Eng. Sci.* **2020**, 60, 2414. <https://doi.org/10.1002/pen.25480>
- [31] M. H. Al-saleh, U. Sundararaj, *J. Polym. Sci. B Polym. Phys.* **2012**, 50, 1356. <https://doi.org/10.1002/polb.23129>
- [32] M. H. Al-Saleh, W. H. Saadeh, U. Sundararaj, *Carbon* **2013**, 60, 146. <https://doi.org/10.1016/j.carbon.2013.04.008>
- [33] M. H. Al-Saleh, *Synth. Met.* **2015**, 205, 78. <https://doi.org/10.1016/j.synthmet.2015.03.032>
- [34] M. H. Al-saleh, *Synth. Met.* **2016**, 217, 322.
- [35] S. K. Chiu, J. Y. Cheng, W. S. Jou, G. J. Jong, S. C. Wang, C. M. Wang, C. S. Lin, T. L. Wu, W. H. Cheng, Electromagnetic shielding of plastic material in laser diode modules, presented at IEEE Electronic Components and Technology Conference, 2001, pp. 645–647, <https://doi.org/10.1109/ECTC.2001.927797>
- [36] M. Arjmand, M. Mahmoodi, G. A. Gelves, S. Park, U. Sundararaj, *Carbon* **2011**, 49, 3430. <https://doi.org/10.1016/j.carbon.2011.04.039>
- [37] M. Arjmand, T. Apperley, M. Okoniewski, U. Sundararaj, *Carbon* **2012**, 50, 5126. <https://doi.org/10.1016/j.carbon.2012.06.053>
- [38] M. H. Zhang, J. K. Chen, *Plast. Rubber Compos.* **2013**, 42, 437. <https://doi.org/10.1179/1743289813Y.0000000063>
- [39] J. M. K. Julia, A. King, R. L. Barton, R. A. Hauser, *Polym. Compos.* **2008**, 29, 421. <https://doi.org/10.1002/pc>
- [40] Z. Fan, C. Zheng, T. Wei, Y. Zhang, G. Luo, *Polym. Eng. Sci.* **2009**, 49, 2041. <https://doi.org/10.1002/pen.21445>
- [41] P. E. A. Tokobaro, N. M. Larocca, E. H. Backes, L. A. Pessan, *Polym. Eng. Sci.* **2021**, 61, 538. <https://doi.org/10.1002/pen.25598>
- [42] A. Shayesteh Zeraati, A. Mende Anjaneyalu, S. P. Pawar, A. Abouelmagd, U. Sundararaj, *Polym. Eng. Sci.* **2021**, 61, 959. <https://doi.org/10.1002/pen.25591>
- [43] S. Zhou, A. N. Hrymak, M. R. Kamal, *Polym. Eng. Sci.* **2018**, 58, E226–E234. <https://doi.org/10.1002/pen.24682>
- [44] S. I. S. Shaharuddin, M. S. Salit, E. S. Zainudin, *Turk. J. Eng. Environ. Sci.* **2006**, 30, 23. <https://doi.org/10.3906/sag-1207-74>
- [45] C. Severance, D. Nobbs, Effect of Processing Parameters on Electrical Properties of Electrically Conductive Composites, presented at ANTEC Proceedings, **2006**, pp. 471–475.
- [46] S. Y. Yang, C. Y. Chen, S. H. Parn, *Polym. Compos.* **2002**, 23, 1003. <https://doi.org/10.1002/pc.10496>
- [47] S. C. Chen, R. Der Chien, P. H. Lee, J. S. Huang, *J. Appl. Polym. Sci.* **2005**, 98, 1072. <https://doi.org/10.1002/app.22241>
- [48] C. S. Chen, W. R. Chen, S. C. Chen, R. Der Chien, *Int. Commun. Heat Mass Transf.* **2008**, 35, 744. <https://doi.org/10.1016/j.icheatmasstransfer.2008.02.006>
- [49] W.-S. Cheng, C.-S. Chen, S.-C. Chen, R.-D. Chien, *Polym.-Plast. Technol. Eng.* **2009**, 48, 216. <https://doi.org/10.1080/03602550802634592>
- [50] M. Mahmoodi, M. Arjmand, U. Sundararaj, S. Park, *Carbon* **2012**, 50, 1455. <https://doi.org/10.1016/j.carbon.2011.11.004>
- [51] A. Ameli, P. U. Jung, C. B. Park. Effects of process variables on through-plane electrical conductivity of injection-molded carbon fiber/polypropylene composite fomas, **2012**.

- [52] N. C. Das, T. K. Chaki, D. Khastgir, *Carbon* **2002**, *40*, 807.  
[https://doi.org/10.1016/S0008-6223\(01\)00229-9](https://doi.org/10.1016/S0008-6223(01)00229-9)

### SUPPORTING INFORMATION

Additional supporting information may be found in the online version of the article at the publisher's website.

**How to cite this article:** L. C. Martins, C. N. Barbosa, S. Silva, P. Bernardo, G. R. Dias, A. J. Pontes, *Polym. Eng. Sci.* **2021**, *61*(10), 2576. <https://doi.org/10.1002/pen.25784>